Geometry and space-time extent of pion emission region at FCC energies

V.A. Okorokov*
National Research Nuclear University MEPhI (Moscow Engineering Physics Institute), Kashirskoe shosse 31, 115409 Moscow, Russian Federation
(Dated: December 6, 2016)

The energy dependence is investigated for a wide set of space-time characteristics derived from Bose – Einstein correlations of secondary pion pairs produced in proton-proton and nucleus-nucleus interactions. Analytic functions suggested for smooth approximations of the energy dependence of emission region parameters demonstrate reasonable agreement with all available experimental results for proton-proton collisions while the approximations correspond to most of experimental data for nucleus-nucleus collisions at energies above 5 GeV. Estimations for a wide set of space-time quantities are obtained for energies for the Future Circular Collider (FCC) project based on the smooth approximations. The space particle densities at freeze-out are derived also from estimations for the volume of the emission region and for total multiplicity at FCC energies. Estimations for charged particle density and its critical value allow the possibility of lasing behavior for secondary pions in nucleus-nucleus collisions at FCC energy. The mathematical formalism is presented for study of the peak shape of correlation function for general case of central-symmetrical Lévy – Feldheim distribution.

PACS numbers: 25.75.Gz - Particle correlations and fluctuations

arXiv:1607.01946v3 [hep-ph] 4 Dec 2016

I. INTRODUCTION

When two energetic particles or nuclei collide, some matter is created in finite space-time volume. This matter volume, often called "fireball", emits particles and space-time extent of the fireball is of fundamental interest for understanding of both the multiparticle production dynamics and the evolution of early Universe. One of the collective effects, namely, particle correlations at low relative momentum represent a unique tool and sensitive probe of the size and the shape of the fireball at the last stage of its evolution (colorless particle emission region). The space-time geometry of particle source can be determined by using a method of interferometry based on the fundamental relation between spin and statistics. The production of identical bosons that are close together in phase space is enhanced by the presence of quantum statistical effect on Bose – Einstein correlations (BEC). The strength and form of the correlation reflects the space-time structure of the source [1]. The most of secondary particles produced in the strong interactions are pions. Thus in the paper correlations between two identical bosons called BEC are studied for secondary charged pions produced in various strong interaction processes[1].

The international project called Future Circular Collider (FCC) is mostly aimed at hadron collider with a centre-of-mass energy $\sqrt{s_{\rm pp}} = 100$ TeV for $p + p$ collisions in a new 100 km tunnel of the CERN accelerator complex and detailed characteristics of various beams for FCC can be found elsewhere [3]. For heavy-ion collisions the relation $\sqrt{s_{\rm NN}} = \sqrt{s_{\rm pp} \times (Z_1 Z_2 / A_1 A_2)}$ gives the energy in centre-of-mass per nucleon-nucleon collision of $\sqrt{s_{\rm NN}} = 39$ TeV for Pb + Pb ($Z = 82$, $A = 208$) and 63 TeV for p + Pb collisions [4, 5]. This project provides a unique opportunity to probe quantum chromodynamics (QCD) in the new energy regime [6]. The one of the most distinguishing features of QCD is the mechanism of color confinement, the physics of which is not fully understood, due, in part, to its theoretical intractability [7]. The confinement mechanism has a physical scale of the order of the proton radius and is especially important at low momentum. Therefore study of source geometry in new energy domain with help of BEC seems important for better understanding of both the equation of state (EOS) of strongly interacting matter and general dynamic features of soft processes. The peak of two-particle Bose - Einstein correlation function (CF) contains the unique experimental information about particle source at freeze-out. The peak shape carries information, in particular, about the possible complex highly irregular geometry of the source [8, 9], the $U_{\rm A}(1)$ symmetry restoration in high energy heavy ion reactions [10] etc. Therefore the development of a general formalism for detailed shape analysis of the peak in BEC CF is relevant for future high-statistics studies at FCC. It should be stressed that on the one hand the BEC leads also to Bose – Einstein condensates responsible for laser, superfluids and superconductors [1]. On the other hand the pion multiplicity at midrapidity $(dN/d\eta)|_{\eta=0}$ is larger than 10^3 in heavy ion collisions in the TeV-energy domain, in particular, at FCC the $(dN/d\eta)|_{\eta=0} \simeq 3600$ in Pb + Pb collisions at $\sqrt{s_{\rm NN}} = 39$ TeV [4]. Therefore the number of pions in a unit value of phase-space may be large enough that these bosons condense into the same quantum state and a pion laser could be created [11, 12]. Thus the paper is focused on the study of azimuthally

* VAOkorokov@mephi.ru; Vitaly.Okorokov@cern.ch

[1] In these reactions the BEC are often called HBT correlations due to analogy with Hanbury-Brown and Twiss effect [2] used in radio astronomy to measure the angular sizes of stellar objects.

integrated BEC of secondary charged pions produced in strong interactions, especially, on the space-time extent of pion emission region and the possible novel features of multiparticle production mechanism (pion laser) at FCC energies. Also the general formalism is suggested for study of shape of correlation peak in detail.

The paper is organized as follows. In Sec. II, definitions of two-particle CF and BEC parameters are described. The Sec. III devotes discussion of energy dependence of pion source extent in $p+p$ and A + A collisions, predictions for wide set of space-time characteristics for pion source in various collisions at FCC energies. The possibility for pion laser in strong interaction processes at FCC energies is considered in Sec. IV. In Sec. V, the generalized parametrization of 3D CF is introduced with help of expansion of central-symmetrical Lévy – Feldheim distribution. Some final remarks are presented in Sec. VI.

II. METHOD AND VARIABLES

The BEC effect is observed as an enhancement in the two-particle CF at low values of some difference constructed from 4-momenta p_i, $i = 1, 2$ or its components of the entering particles, $C_2(p_1, p_2) = \rho(p_1, p_2)/\rho_{\rm ref}(p_1, p_2)$, where the ρ is the two-particle density function, $\rho_{\rm ref}$ is a reference two-particle density function that by construction is expected to include no BEC. Recent study [13] shows that BEC 1D experimental data samples are not enough for study of energy dependence of source parameters in proton-nucleus and nucleus-nucleus collisions. Therefore the present paper is focused on the 3D analysis of BEC in strong interaction processes.

In general phenomenological parametrization of CF with taking into account different forms of corrections on Coulomb final state interaction (FSI) can be written as follows [9]:

$$C^{\rm ph}_{2,(m)}(q,K) = \zeta P^{(m)}_{\rm coul}(q)\big[\zeta^{-1} + \mathbf{K}^{\rm ph}_2(\mathbf{A})\big], \tag{1a}$$

$$\mathbf{K}^{\rm ph}_2(\mathbf{A}) = C^{\rm ph}_{2,(m)}(q,K) - 1, \tag{1b}$$

where $\mathbf{K}_2$ is the cumulant correlation function (cCF), $\zeta = \lambda$ at $m = 1, 2$ and $\zeta = 1$ at $m = 3$ while $m = 1$ corresponds to the standard Coulomb correction, $m = 2$ – the dilution procedure and $m = 3$ – the Bowler – Sinyukov correction, $q \equiv (q^0, \vec{q}) = p_1 - p_2$ is the relative 4-momentum, $K \equiv (K^0, \vec{K}) = (p_1 + p_2)/2$ – the average 4-momentum of particles in pair (pair 4-momentum), $\mathbf{A} \equiv \vec{q}\mathbf{R}^2\vec{q}^{\,T}$ and $\mathbf{R}^2$ are the matrices 3×3, $\vec{q}^{\,T}$ – transposed vector $\vec{q}$, $\forall\ i,j = 1-3 : R^2_{ij} = R^2_{ji}, R^2_{ii} \equiv R^2_i$, where $R_i = R_i(K)$ are parameters characterized the linear scales of the region of homogeneity [14]; the products are taken on space components of vectors, $\lambda(K) = \mathbf{K}_2(0,K), 0 \le \lambda \le 1$ is the parameter which characterizes the strength of correlations called also chaoticity. Different types of Coulomb correction for two-pion correlations are compared in [9]. The space component of pair 4-momentum ($\vec{K}$) is decomposed on longitudinal $k_\parallel = (p_{\parallel,1} + p_{\parallel,2})/2$ and transverse $\vec{k}_\perp = (\vec{p}_{\perp,1} + \vec{p}_{\perp,2})/2$ parts of pair momentum. In the paper the decomposition of Pratt – Bertsch [15] is used for $\vec{q}$ as well as the longitudinal co-moving system (LCMS) frame. The parametrization of the $\mathbf{K}^{\rm ph}_2(\mathbf{A})$ depends on type of distribution which was chosen for emission region [9]. For instance, the lowest order cCF can be written as

$$\mathbf{K}^{\rm ph,0}_{2,\rm G}(\mathbf{A}) = \exp\Big(-\sum_{i,j=1}^{3} q_i R^2_{ij} q_j\Big). \tag{2}$$

for specific case of Gaussian distribution which is one of the most used in BEC study. As known the study of BEC allows the estimation of space-time extent for region of homogeneity which is only some part of whole source. Therefore the BEC parameters $\forall\ i = 1-3 : R_i(K)$ are smaller *a priori* than corresponding scales of whole emission region and consequently the experimental BEC dimensions $R_i(K)$ can be considered as low boundary for corresponding true linear scales of source

$$\forall\ i = 1-3 : R_i(K) = \inf R^{\rm tr}_i(K). \tag{3}$$

For this reason the BEC parameters $\forall\ i = 1-3 : R_i(K)$ are called BEC radii and it is assumed that correlation analysis for pairs of identical particles with low $\langle\vec{k}_\perp\rangle$ provides the R_i which are adequate experimental estimations for space-time extent of whole emission region within the simplest approach at least. It should be noted that azimuthally integrated BEC analysis allows rougher estimations for space-time scales of whole source with increase of collision energy because more intensive collective expansions reduce the sizes of the region of homogeneity more significantly at higher energies. Thus in the present paper the R_i, $i = 1-3$ are considered as source BEC radii with taking into account the relation (3) and influence of collective flows on the quality of this approximation.

In the 3D case and the Pratt – Bertsch coordinate system the space-time extents of the region of homogeneity or, with taking into account the discussion above, whole source is described by the following dimensions: $R_{\rm l}$ is the source size along the beam axis, $R_{\rm o}$ – extent along the $\vec{k}_\perp$ and $R_{\rm s}$ is the source size along the axis perpendicular to those two. Then one can define the geometric mean BEC radius

$$R^3_{\rm m} = \prod_{i={\rm s,o,l}} R_i \tag{4}$$

as well as the difference

$$\delta \equiv R^2_{\rm o} - R^2_{\rm s} \tag{5}$$

which is an important observable especially for some specific cases of 1D hydrodynamics (static, nonflowing source) due to its relation with particle emission duration

$\delta \approx \beta_\perp^2 (\Delta\tau)^2$ [16, 17], where $\beta_\perp = k_\perp/m_\perp$ is the transverse velocity of pair of particles with mass m, $m_\perp^2 = k_\perp^2 + m^2$. Here the scaled geometric mean BEC radius is defined as follows $R_{\rm m}^n = R_{\rm m}/R_{\rm A}$ in accordance with approach suggested in [9, 18], where $\langle R_{\rm A}\rangle = (R_{\rm A_1} + R_{\rm A_2})/2$ is the mean radius for beam nuclei, $R_{\rm A} = r_0 A^{1/3}$ is radius of spherically-symmetric nucleus, $r_0 = (1.25 \pm 0.05)$ fm [19]. The volume of source can be written as follows:

$$V = \begin{cases} (2\pi)^{3/2} R_{\rm s}^2 R_{\rm l}, & \text{(a)} \\ 4\pi R_{\rm m}^3/3, & \text{(b)} \end{cases} \tag{6}$$

where the first case is the standard relation for BEC while the second case corresponds to the simplest approach of spherically symmetric source and it can be useful for future study of pion laser. Thus in the paper the following set of main BEC observables $\mathcal{G}_1 \equiv \{\mathcal{G}_1^i\}_{i=1}^4 = \{\lambda, R_{\rm s}, R_{\rm o}, R_{\rm l}\}$ is under consideration as well as the set of important additional observables which can be calculated with help of BEC radii $\mathcal{G}_2 \equiv \{\mathcal{G}_2^j\}_{j=1}^4 = \{R_{\rm o}/R_{\rm s}, R_{\rm m}, \delta, V\}$. The set of parameters $\mathcal{G}_1$ characterizes the chaoticity of source and its 4-dimensional geometry at freeze-out stage completely.

III. SPACE–TIME EXTENT OF PION SOURCE

In this study experimental BEC data sets are from [20] for $p+p$ and from [18] for A + A collisions.

Dependencies of BEC parameters $\mathcal{G}_1^i(\sqrt{s_{NN}})$, $i = 1-4$ for $p+p$ high energy collisions are shown in Figs. 1a–d respectively. As seen for energy range from Relativistic Heavy Ion Collider (RHIC) to the Large Hadron Collider (LHC) the experimental $\lambda(\sqrt{s_{NN}})$ is close to the constant (Fig. 1a) while the some decrease is observed for experimental $\lambda(\sqrt{s_{NN}})$ deduced from 1D two-pion BEC analyses [21]. The BEC radii increase with collision energy (Fig. 1b–d) more significantly in transverse plane with respect of the beam direction than that for longitudinal direction. Taking into account the view of experimental $\mathcal{G}_1^i(\sqrt{s_{NN}})$, $i = 1-4$ in $p+p$ as well as the detailed study of energy dependence of azimuthally integrated main BEC parameters $\mathcal{G}_1^i$, $i = 1-4$ for charged pions in nucleus-nucleus interactions [18] the following function is used

$$f(\varepsilon) = a_1 \left[1 + a_2 (\ln \varepsilon)^{a_3}\right] \tag{7}$$

for smooth approximation of experimental dependencies $\mathcal{G}_1^i(\sqrt{s_{pp}})$, $i = 1-4$ in $p+p$ interactions. Here $\varepsilon \equiv s_{pp}/s_0$ for $p+p$ or $\varepsilon \equiv s_{NN}/s_0$ for A + A reactions, where $s_0 = 1$ GeV^2. The very limited ensemble of experimental points from 3D Gaussian analyses of $p+p$ does not allow the fit by (7) with all parameters $\forall\, i = 1-3 : a_i$ to be free. In general the various quantities from the set $\mathcal{G}_1$ can show the different behavior as function of $\ln\varepsilon$ [18]. Thus following two views of (7) are used for approximation of experimental points: (i.1) function (7) at fixed value of a_3 which is defined by method of sequential approximations, (i.2) the specific case of (7) at $a_3 = 1.0$. Only statistical uncertainties are available for strength of correlations λ while for each BEC radii $\{\mathcal{G}_1^i\}_{i=2}^4$ fits are made for both the statistical and total errors, where total errors of experimental points include available clear indicated systematic errors added in quadrature to statistical ones. The numerical values of fit parameters are presented in Table I, where the second line for chaoticity parameter λ corresponds to the simplest fit by constant and for each BEC radii – to the approximation by specific case of (7). Approximation curves are shown in Fig. 1a by solid line for specific case of (7) and by dashed line for fit by constant. Figs. 1b–d show the fit results for BEC radii by solid lines for approach (i.1) and by dashed lines for specific case (i.2) with taking into account the statistical errors of experimental points.

In difference with A + A collisions [18] function (7) for both choices of a_3 agrees with experimental $p+p$ data quantitatively and provides reasonable fit qualities even with statistical errors for all BEC parameters from the set $\mathcal{G}_1$ with exception of $R_{\rm s}$. In the last case one can only conclude that fit curve is similar to the general trend of experimental points (Fig. 1b) due to poor fit quality. Account for total errors allows statistically acceptable fit qualities for all main BEC parameters in both approaches (i.1) and (i.2). Furthermore the a_2 is equal to zero within errors for longitudinal BEC radius for (i.2) and consequently the $R_{\rm l}(\sqrt{s_{pp}})$ can be described by constant with $a_1 = (1.57 \pm 0.13)$ fm, χ^2/n.d.f. $= 0.42/2$ in the case of the accounting for total errors. For energy range from RHIC to the LHC fit curves for approaches (i.1) and (i.2) are close to each other for $\mathcal{G}_1^i$, $i = 2-4$ especially for radii $R_{\rm o}$ (Fig. 1c) and $R_{\rm l}$ (Fig. 1d). Nevertheless the fit within approach (i.1) for $R_{\rm o}$ only confirms the $R_{\rm o} \propto \ln\varepsilon$ for statistical errors but other BEC radii show the faster increasing with $\sqrt{s_{pp}}$ especially the $R_{\rm l}$ (Table I). The growth of the $R_{\rm s}$ approaches to the linear behavior in $\ln\varepsilon$ for accounting for total errors but longitudinal radius $R_{\rm l}$ preserves much faster growth with energy increase in this case too. As consequence the method of sequential approximations for a_3 leads to significant improvement of the fit quality with respect to the quantity for approach (i.2) for $R_{\rm s}$ at statistical errors and especially for $R_{\rm s}$ at all considered types of errors. It should be noted the difference between smooth curves obtained within the approaches (i.1) and (i.2) for BEC radii can be much more noticeable for higher energy FCC than that in Fig. 1 which can have a relevant effect on the estimated BEC parameters at FCC.

Dependencies of additional BEC parameters $\mathcal{G}_2^j(\sqrt{s_{NN}})$, $j = 1-4$ for $p+p$ interactions are shown in Figs. 2a–d respectively. Notations of smooth curves correspond to the Fig. 1 namely the solid curves show the results calculated with help of fits of BEC radii within approach (i.1) and dashed lines are for special fits (i.2). As seen curves of both types agree with experimental points reasonably for $R_{\rm o}/R_{\rm s}$ (Fig. 2a) and

TABLE I. Values of fit parameters for approximation of $p+p$ data

BEC	Fit with statistical errors				Fit with total errors			
parameter	a_1	a_2	a_3	χ^2/n.d.f.	a_1	a_2	a_3	χ^2/n.d.f.
λ	0.43 ± 0.06	-0.001 ± 0.012	1.0	$7.0 \times 10^{-4}/1$	–	–	–	–
	0.422 ± 0.004	–	–	$4.9 \times 10^{-4}/1$	–	–	–	–
$R_{\rm s}$	$(6.8 \pm 1.0) \times 10^{-3}$	7.57 ± 0.24	1.21	47.7/1	$(8.0 \pm 1.2) \times 10^{-3}$	7.3 ± 1.0	1.16	0.57/1
	$(2.5 \pm 0.7) \times 10^{-3}$	35 ± 7	1.0	62.6/1	$(1.6 \pm 1.0) \times 10^{-3}$	53 ± 17	1.0	0.72/1
$R_{\rm o}$	0.19 ± 0.08	0.36 ± 0.07	0.97	3.64/1	0.028 ± 0.019	4.1 ± 2.9	0.84	0.11/1
	0.21 ± 0.08	0.29 ± 0.14	1.0	3.71/1	0.19 ± 0.05	0.33 ± 0.10	1.0	0.12/1
$R_{\rm l}$	1.45 ± 0.03	$(9.2 \pm 1.4) \times 10^{-5}$	2.72	$9.4 \times 10^{-9}/1$	1.40 ± 0.12	$(5.7 \pm 2.3) \times 10^{-4}$	2.14	$5.7 \times 10^{-4}/1$
	1.16 ± 0.07	0.030 ± 0.006	1.0	0.35/1	1.2 ± 0.6	0.03 ± 0.06	1.0	$4.9 \times 10^{-4}/1$

$R_{\rm m}$ (Fig. 2b) in total experimentally available energy range. Otherwise the approach (i.1) leads to significant overpredictions for $-\delta$ (Fig. 2c) and V (Fig. 2d) at the LHC energy $\sqrt{s_{NN}} = 7$ TeV while the curves for special case (i.2) agree with experimental points at this energy.

Thus there is significant uncertainty in functional behavior of dependence of experimental BEC parameters on collision energy due to very limited ensemble of 3D experimental data for $p+p$ and future experimental results are important crucially for more definitive conclusion with regard of behavior of dependencies $\mathcal{G}^i_{1,2}(\sqrt{s_{NN}})$, $i = 1-4$.

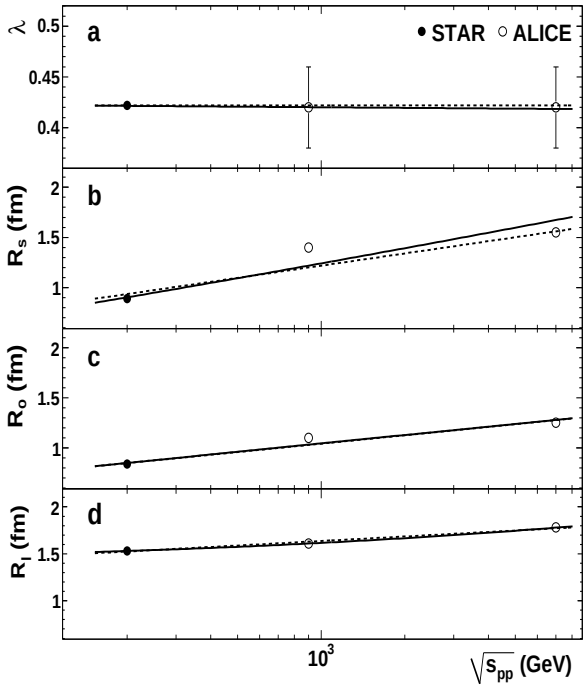

FIG. 1. Energy dependence of the main BEC parameters $\mathcal{G}^i_1$, $i = 1-4$ obtained for 3D Gaussian analyses for $p+p$ collisions at midrapidity and low $\langle k_T \rangle \simeq 0.2$ GeV/c. Errors for experimental points are statistical only. For strength of correlations (a) fit by specific case of (7) at $a_3 = 1.0$ is shown by solid line, the dashed line corresponds to the fit by constant. For BEC radii (b–d) approximations by function (7) are shown by solid lines for case (i.1), dashed lines present the results for linear logarithmic function in the case (i.2).

The pion emission duration $\Delta\tau$ for $p+p$ collisions can be estimated with taking into account the results for $|\delta|$ and kinematic regime for pion pairs under study. The $\langle \beta_\perp \rangle \approx 0.82$ for pion pairs with $\langle k_\perp \rangle \simeq 0.2$ GeV/c as well as for nuclear collisions [18]. Then pion emission duration increases from $\Delta\tau = (0.36 \pm 0.08)$ fm/c at RHIC energy $\sqrt{s_{pp}} = 0.2$ TeV up to the $\Delta\tau = (1.25 \pm 0.12)$ fm/c at the LHC energy $\sqrt{s_{pp}} = 7$ TeV which is highest for available experimental BEC results. Thus the pion emission durations in $p+p$ collisions are smaller significantly than that for nuclear interactions [18] in the energy range from RHIC top up to the LHC.

The energy dependence for BEC parameters from the sets $\mathcal{G}^i_{1,2}(\sqrt{s_{NN}})$, $i = 1-4$ was studied in detail in [18] for nuclear collisions with exception of the $R_{\rm m}$ and corresponding scaled quantity $R^n_{\rm m}$ defined in the present paper. Energy dependence of these additional BEC parameters are obtained with experimental database for nuclear collisions from [18]. Figs. 3, 4 show the experimental $R_{\rm m}(\sqrt{s_{NN}})$ and $R^n_{\rm m}(\sqrt{s_{NN}})$ respectively as well as smooth curves calculated with fit results for BEC radii at $\sqrt{s_{NN}} \geq 5$ GeV from [18]. In Figs. 3, 4 solid curves for $R_{\rm m}(\sqrt{s_{NN}})$ and for $R^n_{\rm m}(\sqrt{s_{NN}})$ respectively are obtained with help of results from fits of BEC radii by general view of (7) and dashed curves correspond to the calculations with fit results for BEC radii for special case of (7) at $a_3 = 1.0$. As seen in Figs. 3, 4 the behavior of smooth curves with respect to each other as well as to the experimental data are quite similar for the $R_{\rm m}$ and $R^n_{\rm m}$. In both cases curves correspond to experimental points reasonably at intermediate energies $10 \lesssim \sqrt{s_{NN}} \lesssim 200$ GeV with excess over experimental points in dip region $5 \lesssim \sqrt{s_{NN}} < 10$ GeV, opposite situation is seen for TeV energies (Figs. 3, 4). In Figs. 3, 4 solid curves are close to dashed ones in total energy range considered especially for $R_{\rm m}$ but onset of the excess of solid curve over dashed one at $\sqrt{s_{NN}} > 1$ TeV for $R_{\rm m}$ (Fig. 3) and at $\sqrt{s_{NN}} > 0.2$ TeV for $R^n_{\rm m}$ (Fig. 4) can lead to a noticeable discrepancy at FCC energy.

As expected, the quantitative comparisons of Figs. 1b-d with Fig. 2b for $p+p$ reactions and Fig. 3 with results for BEC radii R_i, $i = {\rm s, o, l}$ in nuclear collisions [18] show

that $\forall\, i = \mathrm{s,o,l} : R_{\mathrm{m}} \sim R_i$ at qualitative level.

Predictions for values of the BEC observables from sets $\mathcal{G}_{1,2}$ are obtained for suggested types of collisions and energies of the LHC and FCC project [3–5] based on the fit results for the main BEC parameters discussed above and in [18]. Estimations are shown in Table II for fits by function (7) and its specific case at $a_3 = 1.0$ with inclusion of statistical errors of experimental points, the first column for each type of collisions corresponds to the nominal LHC energy and the second column – to the energy of FCC project. One notes the fit by constant predicts $\lambda = 0.422 \pm 0.004$ for the strength of correlations in $p+p$ collisions for both the LHC and FCC energies. Values for all additional BEC parameters $\mathcal{G}_2^j$, $j = 1-4$ are calculated with help of its definitions (4) – (6a) and estimations for BEC radii at some energy. The pion emission duration is derived from $|\delta|$ and kinematic regime for pion pairs under study as well as for $p+p$ at lower energies. Results for asymmetric collisions $p+\mathrm{Pb}$ are obtained with help of fit results for scaled BEC parameters [18] and rough estimation $\langle R_{p\mathrm{Pb}} \rangle = (4 \pm 3)$ fm. In the case of $\mathrm{Pb}+\mathrm{Pb}$ collisions the results for main BEC parameters $\mathcal{G}_1^i$, $i = 1-4$ as well as for $\mathcal{G}_2^j$, $j = 1,4$ and emission duration are from [18], furthermore the brief discussion of estimations for these BEC parameters at the LHC and FCC energies can be also found in the previous studies

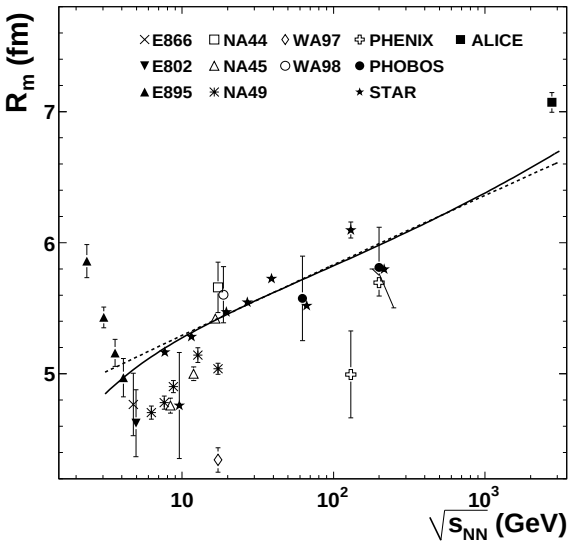

FIG. 3. Energy dependence of R_{m} for secondary charged pions in central heavy ion collisions Au+Au, Au+Pb, Pb+Pb in midrapidity region and at $\langle k_\perp \rangle \simeq 0.2$ GeV/c. Error bars are only statistical (for NA44, total uncertainties). Smooth curves are derived from (4) and the fit results for BEC radii [18] without the point of the WA97 experiment [22]. The solid line corresponds to the fits of BEC radii by function (7) and dashed line – to the fits by specific case $\forall\, i = \mathrm{s,o,l} : R_i \propto \ln \varepsilon$.

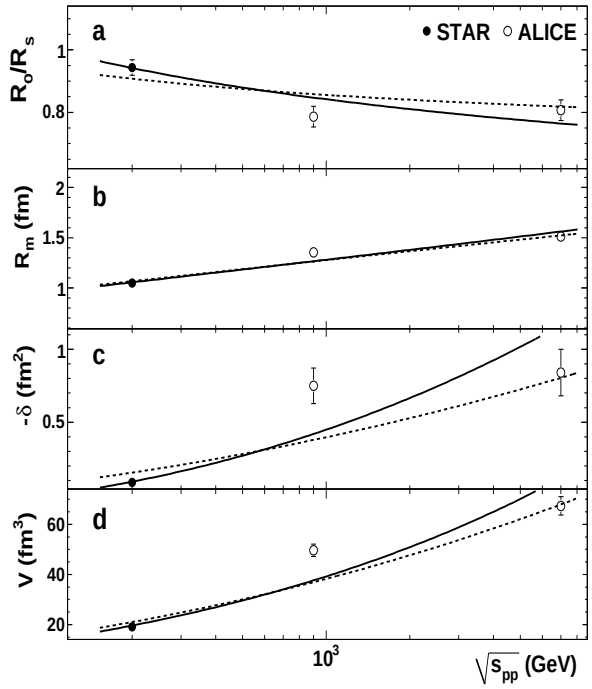

FIG. 2. Energy dependence of the additional BEC parameters $\mathcal{G}_2^j$, $j = 1-4$ for $p+p$ collisions at midrapidity and low $\langle k_T \rangle \simeq 0.2$ GeV/c. Errors for experimental points are statistical only. Smooth curves are calculated with help of fit results for BEC radii, solid lines are from fits of R_i, $i = \mathrm{s,o,l}$ by function (7) in the case (i.1) and dashed lines corresponds to the fits by specific case $R_i \propto \ln \varepsilon$, $i = \mathrm{s,o,l}$.

[18, 20]. As seen from Table II all BEC parameters have values coincided with each other for two approaches (i.1) and (i.2) within errors for corresponding collision energies and types of strong interaction processes. In general estimations for BEC parameters calculated with approach (i.1) do not change from the LHC up to FCC energies within large uncertainties for all collisions under consideration. Proton-proton and nucleus-nucleus collisions are characterized by similar strength of correlations for approach (i.2) for the LHC and FCC energies, the large uncertainty for $p+\mathrm{Pb}$ allows only the qualitative conclusion that λ is somewhat smaller for this collision type than that for $\mathrm{Pb}+\mathrm{Pb}$ in the case of general view of (7) and for $p+p$, $\mathrm{Pb}+\mathrm{Pb}$ within the framework of the approach (i.2). The λ is quite constant for $p+p$ collisions but shows noticeable decrease for heavy ion collisions at increasing of $\sqrt{s_{NN}}$ in the energy range LHC – FCC for fit by specific case of (7) at $a_3 = 1.0$. For $p+\mathrm{Pb}$ the estimation of λ obtained with approach (i.1) at $\sqrt{s_{NN}} = 5.02$ TeV agrees rather well with experimental result [23] while the approach (i.2) underpredicts the strength of correlations at the LHC energy. Furthemore estimations for BEC radii of pion source produced in $p+\mathrm{Pb}$ collisions at $\sqrt{s_{NN}} = 5.02$ TeV (Table II) agree with experimental results [23, 24] within large errors. The space scales are about 2 fm in $p+p$, about 4 – 5 fm in $p+\mathrm{Pb}$ and 6 – 9 fm in $\mathrm{Pb}+\mathrm{Pb}$ collisions for pion source at FCC energies. In the case of estimations for BEC radii obtained with general view of (7) large uncertainties do not

TABLE II. Estimations for space-time characteristic of pion source at the LHC and FCC energies

parameter	$p+p$, $\sqrt{s_{pp}}$ (TeV)		$p+\mathrm{Pb}$,$\sqrt{s_{NN}}$ (TeV)		$\mathrm{Pb}+\mathrm{Pb}$,$\sqrt{s_{NN}}$ (TeV)	
	14	100	5.02	63	5.52	39
			from fits by approach (i.1)			
λ	–	–	0.16 ± 0.19	0.05 ± 0.22	0.41 ± 0.03	0.40 ± 0.03
R_s, fm	1.8 ± 0.3	2.3 ± 0.4	3.9 ± 2.9	5 ± 4	6.8 ± 1.9	8 ± 3
R_o, fm	1.4 ± 0.6	1.6 ± 0.7	3.5 ± 2.6	3.6 ± 2.7	6.3 ± 1.0	6.4 ± 1.0
R_l, fm	1.85 ± 0.07	2.12 ± 0.11	4 ± 3	5 ± 3	7.6 ± 1.5	8.1 ± 1.6
$R_\mathrm{o}/R_\mathrm{s}$	0.7 ± 0.4	0.9 ± 1.0	0.7 ± 0.7	0.7 ± 0.7	0.9 ± 0.3	0.8 ± 0.3
R_m, fm	1.67 ± 0.27	2.0 ± 0.3	3.9 ± 1.7	4.4 ± 1.9	6.9 ± 0.9	7.6 ± 1.2
δ, fm^2	-1.5 ± 2.0	-2.7 ± 2.9	-3 ± 29	-20 ± 50	-6 ± 29	-30 ± 60
$\Delta\tau$, fm/c	1.5 ± 1.0	2.0 ± 1.1	2 ± 11	5 ± 7	3 ± 7	7 ± 7
V, fm^3	$(1.0 \pm 0.3) \times 10^2$	$(1.8 \pm 0.5) \times 10^2$	$(1.0 \pm 1.7) \times 10^3$	$(2 \pm 3) \times 10^3$	$(6 \pm 3) \times 10^3$	$(9 \pm 8) \times 10^3$
			from fits by approach (i.2)			
λ	0.42 ± 0.11	0.42 ± 0.13	0.097 ± 0.004	–	0.362 ± 0.009	0.315 ± 0.011
R_s, fm	1.7 ± 0.7	2.0 ± 0.8	3.3 ± 2.4	3.5 ± 2.6	5.79 ± 0.10	6.11 ± 0.12
R_o, fm	1.4 ± 0.7	1.6 ± 0.9	3.6 ± 2.6	3.7 ± 2.7	6.49 ± 0.12	6.74 ± 0.15
R_l, fm	1.82 ± 0.17	1.96 ± 0.20	5 ± 3	5 ± 4	8.20 ± 0.16	9.04 ± 0.19
$R_\mathrm{o}/R_\mathrm{s}$	0.8 ± 0.5	0.8 ± 0.5	1.1 ± 1.1	1.1 ± 1.1	1.12 ± 0.03	1.10 ± 0.03
R_m, fm	1.6 ± 0.4	1.9 ± 0.4	3.7 ± 1.6	4.0 ± 1.7	6.75 ± 0.07	7.19 ± 0.09
δ, fm^2	-1 ± 3	-2 ± 4	2 ± 25	1 ± 27	8.7 ± 2.0	8.2 ± 2.4
$\Delta\tau$, fm/c	1.2 ± 1.9	1.5 ± 2.1	2 ± 11	1 ± 14	3.6 ± 0.4	3.5 ± 0.5
V, fm^3	80 ± 60	$(1.3 \pm 1.0) \times 10^2$	$(0.8 \pm 1.3) \times 10^3$	$(1.0 \pm 1.6) \times 10^3$	$(4.32 \pm 0.17) \times 10^3$	$(5.31 \pm 0.23) \times 10^3$

allow the definite conclusion and one can see qualitative indication only that R_o is some smaller than other radii in all collision types for both the LHC and FCC energies. For estimations based on the special case of (7) with $a_3 = 1.0$ there is noticeable increase of all BEC radii for transition from the LHC to FCC energy in heavy ion collision (Table II). As consequence the R_m and V is larger at $\sqrt{s_{NN}} = 39$ TeV than that at the LHC energy $\sqrt{s_{NN}} = 5.52$ TeV. Spread of values of BEC radii leads to significant uncertainties for estimations of additional space-time parameters especially for extremely asymmetric $p+\mathrm{Pb}$ collisions for which the large error for $\langle R_{p\mathrm{Pb}} \rangle$ increases greatly uncertainties for BEC quantities in Table II. Consequently the volume of the pion source can be roughly estimated as about 200 fm^3 in $p+p$, 2000 fm^3 in $p+\mathrm{Pb}$ and 10^4 fm^3 in $\mathrm{Pb}+\mathrm{Pb}$ collisions at FCC energies in comparison with 100 fm^3 in $p+p$, 1000 fm^3 in $p+\mathrm{Pb}$ and 6000 fm^3 in $\mathrm{Pb}+\mathrm{Pb}$ at the nominal LHC energies. These estimations indicate the consistent growth of V for transition from the small system collisions to the $\mathrm{Pb}+\mathrm{Pb}$. For approach (i.1) estimations for all parameters $\mathcal{G}_2^j$, $i = j - 4$ and for emission duration do not depend on energy in the range LHC – FCC for all types of collisions within errors. This conclusion is also valid for approach (i.2) with exception of the R_m and V for $\mathrm{Pb}+\mathrm{Pb}$ discussed above. It should be noted that weak change of main BEC parameters $\mathcal{G}_1^i$, $i = 1 - 4$ is qualitatively expected for energy domain from the LHC up to FCC because of general trends of available experimental points and consequent slow logarithmic increase with collision energy for smooth analytic functions used in the present analysis as well as in [18, 20].

IV. PION LASER AT FCC ENERGIES

Results shown above for space-time extent of pion emissions region allow the study of possibility of Bose–Einstein condensation with consequent formation of pion laser in high energy strong interaction processes. The key quantity is the charged particle density which is defined as follows:

$$n_\mathrm{ch} = N_\mathrm{ch}/V, \tag{8}$$

where N_ch is the total charged particle multiplicity and V is the source volume at freeze-out stage. The critical density n_ch^c can be calculated with help of (8) and transition to the critical total multiplicity $N_\mathrm{ch} \to N_\mathrm{ch}^\mathrm{c}$. The last multiplicity parameter was derived for 1D thermal Gaussian distribution in [11]. Within the 3D Gaussian parametrization for source the following relation is suggested

$$N_\mathrm{ch}^\mathrm{c} = \eta^{-1} \left[(\Delta R_\mathrm{m})^2 + \sqrt{(p_0 R_\mathrm{m})^2 + 0.25} \right]^{3/2}. \tag{9}$$

Here $\eta = 0.25$ is the fraction of the pions to be emitted from a static Gaussian source, $\Delta = 0.25$ GeV/c is a momentum spread and $p_0/T = p^2/2\Delta^2$ [11], T – source temperature supposed equal to the parameter value at chemical freeze-out, it is suggested $p \approx 3T$ [25]. It should be emphasized that there are no qualitative studies of $T(\sqrt{s_{pp}})$ for $p+p$ collisions so far but set of results for mean multiplicity and the pseudorapidity density at midrapidity for charged particles in various collisions [26, 27] as well as recent results for deconfinement in small system [28, 29] indicate remarkable similarity

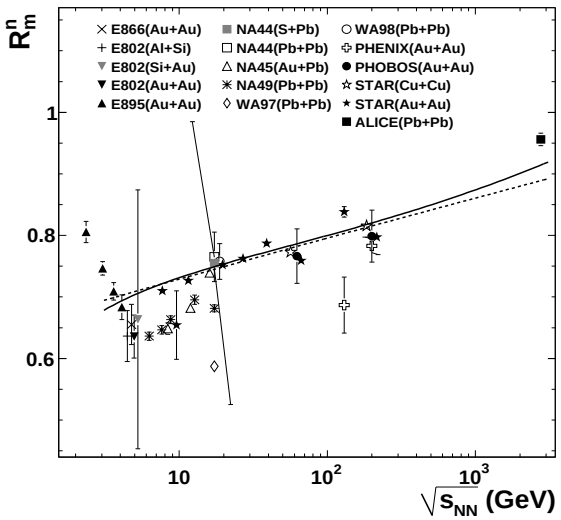

FIG. 4. Energy dependence of scaled $R_{\rm m}^n$ for secondary charged pions in various nucleus-nucleus collisions at $\langle k_\perp \rangle \simeq 0.2$ GeV/c. Experimental results are shown for central collisions (for minimum bias event in the case of E802 for Al+Si), for pairs of π^- mesons (in the cases of ALICE and STAR for both the Cu+Cu and Au+Au at $\sqrt{s_{NN}} = 7.7 - 62.4$ and 200 GeV, for $\pi^\pm\pi^\pm$ pairs, E802 for Al+Si, NA44 for S+Pb, for pairs of π^+ mesons) and for standard Coulomb correction $P_{\rm C}^{(1)}(q)$ (in the cases of ALICE, NA44, NA45, PHOBOS, STAR for both the Cu+Cu and Au+Au at $\sqrt{s_{NN}} = 7.7, 11.5 - 62.4$ and 200 GeV, for correction $P_{\rm C}^{(3)}$). Statistical errors are shown (for NA44, total uncertainties). Smooth curves are derived from fit results for scaled BEC radii [18]. The solid line corresponds to the fits of scaled BEC radii by function (7) and dashed line – to the fits by specific case $\forall\, i = {\rm s,o,l} : R_i^n \propto \ln\varepsilon$.

of both the bulk and the thermodynamic properties of strongly interacting matter created in high energy $p+p$ / $\bar{p}+p$ and A + A collisions. Therefore the hypothesis is suggested for similar energy dependence of T in both the $p+p$ and the A + A interactions with taking into account $\sqrt{s_{pp}} \simeq 3\sqrt{s_{NN}}$ [26, 27] and consequently the analytic energy dependence of T from [30] is used for all types of strong interaction processes considered in this Section. Thus appropriate analytic function is derived for energy dependence of $N_{\rm ch}^{\rm c}$. Also $N_{\rm ch}$ vs collision energy in (8) is defined by some smooth approximations which are specified below for $p+p$ and A + A collisions. Experimental estimations for V available in the Fig. 2e for $p+p$ and in [18] for A + A collisions can be used for calculations of $n_{\rm ch}$ at certain energies. The results of such calculations are called experimental points and marked by symbols in Figures 5 and 6 below in the sense that BEC measurements are used in these cases. As seen from Table I for $p+p$ and from [18] for heavy ion collisions the smooth energy dependence of source volume can be calculated with help of the fits of BEC radii by (ii.1) general function (7) as well as (ii.2) by specific case $R_i \propto \ln\varepsilon$, $i = {\rm s,l}$. The relation (6a) for source volume is used in (8) for experimental estimations as well as for calculations of smooth energy dependence of $n_{\rm ch}$ in both the $p+p$ and the A + A collisions. On the other hand it seems reasonable to use the equation (6b) for estimation of critical charged density because the relation (9) with $R_{\rm m}$ is only available. Taking into account the qualitative relation between $R_{\rm m}$ and 3D BEC radii shown above one expects that the difference of numerical factors for two definition of V (6) provides additional uncertainty $\sim 3\sqrt{\pi/2}$ in the ratio $n_{\rm ch}/n_{\rm ch}^{\rm c}$. Therefore theoretical investigations are essential for quantitative account for geometry of source and decrease of uncertainty due to calculation of volume of emission region. As it follows from (3) and discussion in the Sec. II the relation (8) defines the upper boundary for true value of charged particle density

$$n_{\rm ch} = \sup n_{\rm ch}^{\rm tr} \tag{10}$$

strictly speaking and possibly the discrepancy between estimation from (8) and $n_{\rm ch}^{\rm tr}$ will be increased with growth of collision energy due to intensification of longitudinal and radial collective flows. During the recent years the collectivity in small colliding systems are under intensive theoretical [31] and experimental studies [32] but the results obtained already mean that the statement above is valid for $p+p$ interactions as well as for nucleus-nucleus collisions in TeV-energy domain at least. In general one can assume the weaker dependence of $n_{\rm ch}^{\rm c}$ on space-time parameters of particle source than that for $n_{\rm ch}$ due to BEC radius in (9). The uncertainties of $N_{\rm ch}$ calculated by standard way from errors of fit parameters are attributed as statistical errors. The statistical uncertainties for $N_{\rm ch}^{\rm c}$ are estimated by standard way at assigned relative error $\delta\Delta = 0.05$ and with taking into account the errors for fits of $R_{\rm m}$ and T used while systematic uncertainties are deduced by varying of η within the range $\eta = 0.20 - 0.30$ only. The statistical errors of V propagated from corresponding uncertainties of BEC radii are only taken into account below.

Total charged multiplicity $N_{\rm ch}^{\rm pp}$ is calculated within various approaches [27, 33, 34]. In Fig. 5 energy dependence is shown for $n_{\rm ch}^{\rm pp}$ as well as for critical particle density. It should be noted that in the case of $p+p$ collisions minimum-bias events are used in the BEC analyses [35, 36] and these events correspond to the non-singly diffractive (NSD) $p+p$ collisions at $\sqrt{s_{pp}} = 0.2$ TeV [28] as well as at the LHC energies [37, 38]. Thus experimental points are obtained for $N_{\rm ch}^{\rm pp}$ calculated with hybrid approximation [27]. The thick solid and dashed lines correspond to the source volume within approach (ii.1) and thin lines – to the V from case (ii.2). In Fig. 5 results for $n_{\rm ch}^{\rm pp}$ are shown by solid lines for hybrid approximation of total charged multiplicity [27] and dashed lines are deduced with $N_{\rm ch}^{\rm pp}$ within 3NLO pQCD approach [33] at $\sqrt{s_{pp}} \simeq 0.35\sqrt{s_{ee}}$ [26, 39] and parameters from [40] for number of colors $N_c = 3$. Available experimental estimations show almost constant $n_{\rm ch}^{\rm pp} \simeq 1$. Smooth curves agree with experimental points reasonably for any approximation of $N_{\rm ch}^{\rm pp}$ and V. As seen the differences be-

tween various approaches for each of the two parameters are small up to the LHC energy and increase for FCC noticeably. The dependence of critical particle density $n_{\rm ch}^{\rm c,pp}(\sqrt{s_{pp}})$ shown by dotted line decreases with energy. The statistical ± 1 s.d. band limits are drawn by thin dotted line while this large uncertainty is mostly dominated by the precision of BEC parameters of emission region. The systematic ± 1 s.d. boundaries are shown by heavy grey lines. As seen from Fig. 5 the $n_{\rm ch}$ is smaller than its critical value in $p+p$ collisions up to FCC energy $\sqrt{s_{pp}} = 100$ TeV for any approaches for total charged multiplicities and V under study. This conclusion is valid even with taking into account large statistical uncertainties. Thus one can not expect the kind of lasing behavior for secondary pions in $p+p$ collisions within the present approach.

One can note the coincidence between the experimental values of $N_{\rm ch}$ in p+p and $\bar{p}$+p collisions at energies 0.2 and 0.9 TeV and general smooth energy dependence of $N_{\rm ch}$ for NSD events in the interactions under discussion [38]. Also reasonable agreement is observed for pseudorapidity density $dN_{\rm ch}/d\eta$ measured in $p+p$ [37, 38, 41] and $\bar{p}+p$ [42] interactions at energies indicated above. But there are no 1D BEC analyses with Gaussian model in

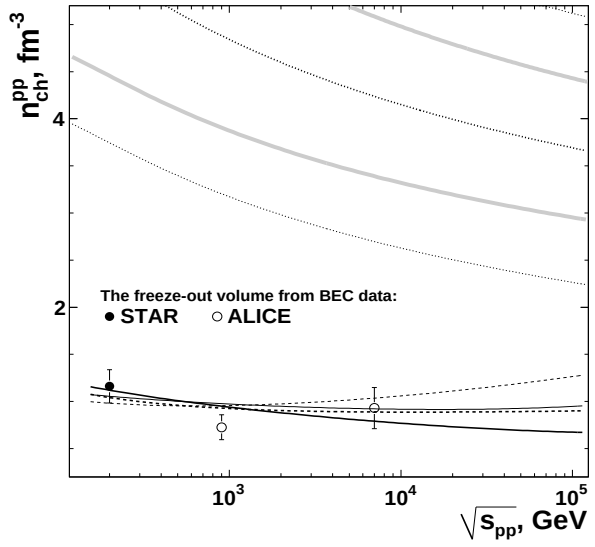

FIG. 5. Energy dependence of estimations for charged particle density and for critical one in $p+p$ collisions. Points are calculated with help of the hybrid function for N_{ch} [27] and the experimental estimations for V and uncertainties for points are propagated from statistical errors of measurements and fits used. Solid lines correspond to the hybrid approximation of N_{ch} [27] and dashed lines are for 3NLO pQCD equation [33] while thick lines show results with V calculated with the fits of BEC radii by (7) in the case (ii.1) and thin lines – with the fits by specific case $R_i \propto \ln\varepsilon$, $i = {\rm s,l}$. Critical charged particle density is shown by dotted line with its statistical uncertainty levels represented by thin dotted lines. The heavy grey lines correspond to the systematic ± 1 s.d. of $n_{\rm ch}$ calculated by varying of η on ± 0.05.

$\bar{p}+p$ collisions at $\sqrt{s_{\bar{p}p}} = 0.2$ and 0.9 TeV. Furthermore the quantitative comparison of BEC results from $p+p$ to those from $\bar{p}+p$ collisions is difficult for 1D case due to limited ensemble of experimental results in the last case [13] and noticeable difference between collision energies in $p+p$ and $\bar{p}+p$ for available BEC measurements; there is no BEC analysis with 3D Gaussian model for $\bar{p}+p$ so far. On qualitative level close values for multiplicity quantities can be expected in $p+p$ and $\bar{p}+p$ collisions in particular at energies about 2 TeV while the 1D BEC Gaussian radius for pion source in $\bar{p}+p$ at $\sqrt{s_{\bar{p}p}} = 1.8$ and 1.96 TeV [43] is significantly larger than that from $p+p$ at $\sqrt{s_{pp}} = 2.36$ TeV [44]. Therefore the $n_{\rm ch}$ is expected smaller in $\bar{p}+p$ than that in $p+p$ collisions at least in TeV-energy domain at close values of critical quantity due to its weaker dependence on space-time extent of particle source. Thus the pion lasers seem impossible in high-energy $\bar{p}+p$ collisions within the rough assumptions.

As discussed above the estimations of space-time extent of pion source are characterized by large uncertainties moreover development of equation for critical parameters for multidimensional (3D) case seems important for improvement of precision of studies and for more certain conclusions. The future quantitative experimental and theoretical investigations are essential for verification of the results shown above and possibility of novel coherent effects in different types of collisions in high energy domain.

Total charged multiplicity $N_{\rm ch}^{\rm AA}$ is calculated with hybrid equations [27, 34]. Fig. 6 demonstrates energy dependence for both the $n_{\rm ch}^{\rm AA}$ and the critical particle density where smooth approximation for $n_{\rm ch}^{\rm AA}$ is shown by solid line for hybrid approximation of total charged multiplicity [27] and by dashed line for $N_{\rm ch}^{\rm AA}$ from [34], and experimental points are obtained for $N_{\rm ch}^{\rm AA}$ calculated with equation from [34]. Both the curves for $n_{\rm ch}^{\rm AA}$ and experimental points are deduced with mean number of participant $\langle N_{\rm part}\rangle = 382.8 \pm 3.1$ which corresponds to the 0–5% central Pb + Pb collisions [34]. This simplest approach seems reasonable because heavy ion collisions are only considered in Fig. 6. The source volume is calculated within approach (ii.1) and results for BEC radii in nuclear collisions [18]. Experimental points for $n_{\rm ch}^{\rm AA}$ increase with $\sqrt{s_{NN}}$ and agree reasonably with smooth curves for both parameterizations of total charged multiplicity under consideration. Comparison between particle densities in $p+p$ (Fig. 5) and A + A (Fig. 6) strong interaction processes indicates the enhancement of $n_{\rm ch}^{\rm AA}$ over $n_{\rm ch}^{\rm pp}$ starting with RHIC energy 200 GeV per nucleon-nucleon pair furthermore this enhancement increases with growth of collision energy. The critical particle density $n_{\rm ch}^{\rm c,AA}$ shown by dotted line depends weakly on $\sqrt{s_{NN}}$ in nuclear collisions. In Fig. 6 the line types for statistical and systematic ± 1 s.d. band limits are the same as well as for corresponding smooth curves for $p+p$ collisions (Fig. 5). The statistical uncertainty driven by the precision of BEC parameters of emission region in-

creases noticeably for multi-TeV region $\sqrt{s_{NN}} \gtrsim 10$ TeV in A + A interactions. The situation changes dramatically with transition from $p + p$ to nuclear collisions at high energies. As seen from Fig. 6 the following relation $n_{\rm ch}^{\rm AA} \approx n_{\rm ch}^{\rm c,AA}$ is valid at RHIC and the LHC energies within wide uncertainty band for critical value of charged particle density. Furthermore there is clear enhancement of smooth curves for $n_{\rm ch}^{\rm AA}$ over $n_{\rm ch}^{\rm c,AA}$ at $\sqrt{s_{NN}} \gtrsim 10$ TeV with taking into account large statistical uncertainty for $n_{\rm ch}^{\rm c,AA}(\sqrt{s_{NN}})$. Thus one can expect the appearance of novel effects dominated by Bose – Einstein condensation in nucleus-nucleus collisions at FCC energy. In particular, Fig. 6 indicates the possibility for pion laser effect in heavy ion collisions at $\sqrt{s_{NN}} \gtrsim 10$ TeV within the approach under study.

With theory point of view the conception of the pion laser was intensively studied within the framework of the model of independent factorized sources [11, 12, 45] as well as in the model of disoriented chiral condensate (DCC) decay [46]. On the other hand possible experimental signatures of Bose – Einstein condensation, in particular, the pion laser effect in heavy ion collisions at FCC energy should be the subject of future detailed investigations. Here one notes the following experimental signatures of Bose – Einstein condensation. In general, one can expects enhancement of high-multiplicity events [11, 12] and the decrease of chaoticity parameter derived from two-particle BEC analysis due to amplification of coherent particle production [47]. The effects of multiboson symmetrization regarding isospin fluctuations can manifest itself through enhancement of the events with anomalous isospin imbalance like CENTAURO events in high-energy cosmic ray [11, 12]. The shrinkage of the BEC radius is the more specific prediction within the model of the DCC decay when the Bose – Einstein condensation takes place [46]. This effect potentially represents one of the most pronounced features of the pion laser, because the available experimental BEC radii show smooth increase with collision energy both in the $p + p$ interactions (Fig. 1) and the heavy ion collisions [18, 20].

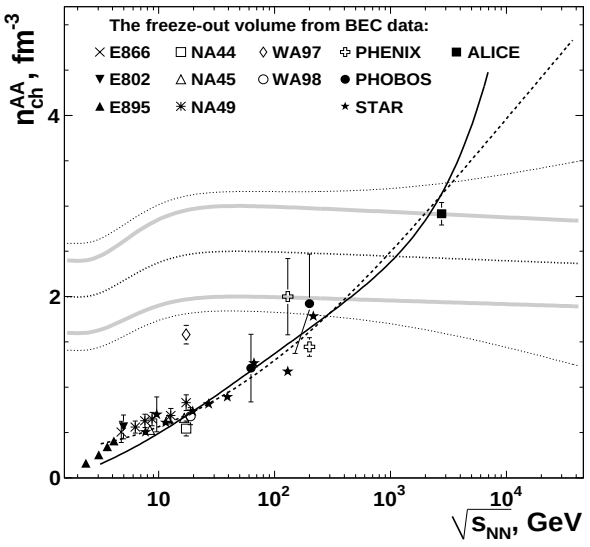

FIG. 6. Energy dependence of estimations for charged particle density and for critical one in A + A collisions. Points are calculated with help of the hybrid function for N_{ch} [34] and the experimental estimations for V and uncertainties for points are propagated from statistical errors of measurements and fits used. Solid line corresponds to the hybrid approximation of N_{ch} [27] and dashed line is for parametrization of total charged multiplicity from [34]. Critical charged particle density is shown by dotted line with its statistical uncertainty levels represented by thin dotted lines. The heavy grey lines correspond to the systematic ±1 s.d. of $n_{\rm ch}$ calculated by varying of η on ±0.05.

V. STUDY OF CORRELATION PEAK SHAPE

The accelerator parameters within the FCC project [3–5] open the new possibility for detailed study of peak structure for two-particle BEC correlation function. The peak of CF is described by $\mathbf{K}_2^{\rm ph}(\mathbf{A})$. In general there is rich class of random processes with additive stochastic variables for which (i.e. for these processes) there are finite distributions but the Central Limit Theorem (CLT) in the traditional (Gaussian) formulation is not valid. The class of random processes under consideration are characterized by large fluctuations, power-law behavior of distributions in the range of large absolute values of random variables, non-analytic behavior of characteristic function of the probability distribution for small values of its arguments [48]. In mathematical statistics and probability theory the class of such distributions are called as stable (on Lévy) distributions[2] [49]. The general stable distribution is described by four parameters: an index of stability (or Lévy index) $\alpha \in (0, 2]$, a parameters of skewness β, scale γ and location δ. These distributions satisfy requirements of generalized Central Limit Theorem (gCLT) and self-similarity[3]. Therefore the detail investigation of the shape of correlation peak has to do with verification of hypothesis of possible self-affine fractal-like geometry of emission region. At present the study of Lévy – Feldheim distributions is the advanced region of mathematics but the specific case of central-symmetrical stable distributions is known in more detail [50]. Just this subclass of stable distributions is most important on the point of view of investigation for BEC. In this case the application of subset of non-isotropic central-symmetrical Lévy – Feldheim distributions [51] seems reasonable be-

[2] In literature for physics and mathematics the multidimensional distributions included in the class are called as Lévy – Feldheim distributions.

[3] The applications of stable distributions in the physics of fundamental interactions and, in particular, for correlation femtoscopy are described, for example, in [17].

cause the projections of the 3D relative momentum $\vec{q}$ are independent random variables.

The multidimensional generalized parametrization of n-th order for CF (1) can be written as follows [9]:

$$C_2^{\mathrm{ph},n}(q,K) = \xi_1(q,K)\left[1+\xi_2(q,K)\mathbf{K}_2^{\mathrm{ph},n}(\mathbf{A})\right], \tag{11a}$$

$$\mathbf{K}_2^{\mathrm{ph},n}(\mathbf{A}) = \mathbf{K}_2^{\mathrm{ph},0}(\mathbf{A})\prod_{i=1}^{3}\prod_{j=1}^{3}\left[1+\sum_{m=1}^{n} g_m h_m(A_{ij})\right], \quad \text{at } n \geq 1. \tag{11b}$$

where $\mathbf{K}_2^{\mathrm{ph},n}$ – phenomenological parametrization of n-th order for cCF (2), functions $\xi_{1,2}(q,K)$ take into account formally all corrections on degree of source chaoticity, final state interactions, etc. The experimental and theoretical investigations in the field of BEC allow us to derive some approach for cumulant two-particle function (2) in the lowest order. Within the framework of the subset of non-isotropic central-symmetrical Lévy – Feldheim distributions the most general parametrization of $\mathbf{K}_{2,\mathrm{L}}^{\mathrm{ph},0}$ can be given by

$$\mathbf{K}_{2,\mathrm{L}}^{\mathrm{ph},0}(\mathbf{A}) = \prod_{i=1}^{3}\prod_{j=1}^{3}\mathbf{K}_{2,\mathrm{L}}^{\mathrm{ph},0}(A_{ij}) = \exp\left(-\sum_{i,j=1}^{3}|A_{ij}|^{\alpha/2}\right), \quad \mathbf{K}_{2,\mathrm{L}}^{\mathrm{ph},0}(x) = \exp(-|x|^{\alpha/2}). \tag{12}$$

Here were take into account that $x \equiv (q_i R_i)^2$, $i = \mathrm{l},\mathrm{o},\mathrm{s}$ for correlation femtoscopy, the products are on the space components of vectors. The $\{h_n(x)\}|_{n=0}^{\infty}$ is the closed system of orthogonal polynomials in the Hilbert space $\mathcal{H}$: $\int dx\mathbf{K}_2(x)h_n(x)h_m(x) = \delta_{nm}$, $g_n = \int dx\mathbf{K}_2(x)h_n(x)$. The system $\{h_n(x)\}|_{n=0}^{\infty}$ for exponential weight function can be derived with the help of the following recurrent relations $a_1h_1(x) = (x-b_0)h_0(x)$, $a_{n+1}h_{n+1}(x) = (x-b_n)h_n(x) - a_{n-1}h_{n-1}(x), n = 1,2,...$ [52] and moments $\mu_n = \int_{-\infty}^{\infty} dx x^n \exp(-|x|^{\gamma}) = 2\gamma^{-1}\Gamma\left(\gamma^{-1}[n+1]\right)$, $n \geq 0$, $\gamma > 0$ [53]. Here $\forall\ n \geq 0 : b_n = \tilde{H}_{n+1}H_{n+1}^{-1} - \tilde{H}_nH_n^{-1}$; $\forall\ n > 0 : a_n = H_n^{-1}\sqrt{H_{n-1}H_{n+1}}$, and $H_n, \tilde{H}_n$ are the following determinants:

$$H_n = \begin{vmatrix} \mu_0 & \dots & \mu_{n-1} \\ \vdots & & \vdots \\ \mu_{n-1} & \dots & \mu_{2n-2} \end{vmatrix}, \tilde{H}_n = \begin{vmatrix} \mu_0 & \dots & \mu_{n-2} & \mu_n \\ \vdots & & \vdots & \vdots \\ \mu_{n-1} & \dots & \mu_{2n-3} & \mu_{2n-1} \end{vmatrix},$$

$H_0 = 1$ and $\tilde{H}_0 = 0$, the $h_0(x) = \mathrm{const} > 0$ is defined by normalization which is chosen for system $\{h_n(x)\}|_{n=0}^{\infty}$ under consideration. The clear view of $h_n(x)$ can be found, for instance, in [54] for few lowest orders n at normalization $h_0(x) = 1$. The specific cases $\alpha = 1$ and $\alpha = 2$ correspond to Cauchy and Gauss distributions respectively which are mostly used in the correlation femtoscopy. For the first case the Laguerre polynomials, $L_n(x)$, are used as $\{h_n(x)\}|_{n=0}^{\infty}$; the Hermite polynomials, $H_n(x)$, are chosen as the closed system of orthogonal polynomials for the second specific case [55].

The generalized parametrization (11) contains the important physical information with regard of the possible high irregular geometry of emission region and dynamics of its creation and it is additional with respect to information derived for sets $\mathcal{G}_{1,2}$ of space-time parameters based on traditional Gaussian parametrization. At now there are a few studies [56] which used the formalism outlined above for specific case of Gaussian distribution only. But these investigations confirm already the importance of detailed analysis of peak shape of CF. Thus high statistics and parameters of multiparticle final state for FCC energies allow us the qualitative study of complex geometry of emission region for secondary pions.

VI. SUMMARY

The following conclusions can be obtained by summarizing the results of the present study.

Energy dependence is investigated for main BEC parameters from the set $\mathcal{G}_1$ derived in the framework of 3D Gaussian approach in $p+p$ collisions as well as for the set of important additional observables $\mathcal{G}_2$. Analytic function is suggested for approximation of energy dependence of main BEC parameters. The fits demonstrate statistically acceptable qualities for λ and for most radii even for taking into account statistical errors of experimental points. Smooth curves calculated for energy dependence of the set $\mathcal{G}_2$ of additional BEC parameters agree with corresponding experimental data at least of qualitative level. The estimation of emission duration of pions in $p+p$ collisions increases from about 0.4 fm/c at RHIC

energy up to 1.3 fm/c at the LHC energy. Estimations are obtained for wide set of space-time characteristics of pion source at FCC energies on the basis of the fit results for $p+p$ and nulceus-nucleus collisions. The pion source is characterized by linear sizes about 2 fm in $p+p$, about 4 – 5 fm in $p+\mathrm{Pb}$ and 6 – 9 fm in $\mathrm{Pb}+\mathrm{Pb}$ collisions at FCC energies. Volume of pion source at freeze-out is estimated from few hundreds of fm^3 in $p+p$ through few thousands of fm^3 in $p+\mathrm{Pb}$ up to 10^4 fm^3 in $\mathrm{Pb}+\mathrm{Pb}$ collisions at FCC energies.

The charged particle density and its critical value is investigated for high energy $p+p$ and $\mathrm{A}+\mathrm{A}$ collisions. The experimental dependence $n_{\mathrm{ch}}^{\mathrm{pp}}(\sqrt{s_{pp}})$ is almost flat and it describes by smooth curves reasonably for various parameterizations of total charged particle multiplicity. The $n_{\mathrm{ch}}^{\mathrm{c,pp}}(\sqrt{s_{pp}})$ decreases with energy nevertheless the estimations of critical value are larger significantly than charged particle density up to FCC energy. Therefore one can not expect the Bose – Einstein condensation and appropriate effects for secondary pions in $p+p$ collisions at FCC within the present approach. The charged particle density is noticeably larger in heavy ion collisions than that in $p+p$ at similar collision energies. The experimental dependence $n_{\mathrm{ch}}^{\mathrm{AA}}(\sqrt{s_{NN}})$ increases with energy in difference with $p+p$ reactions. Smooth curves calculated for various approaches of total charged particle multiplicity agree with experimental points. The situation is dramatically different in high energy nucleus-nucleus collisions with respect to the $p+p$ case. The charged particle density is in the range of estimations of critical parameter within its large uncertainties from the RHIC energy $\sqrt{s_{NN}} = 0.2$ TeV up to the LHC $\sqrt{s_{NN}} = 2.76$ TeV which is highest for experimentally available BEC results in nucleus-nucleus collisions. Furthermore there is clear enhancement of values estimated for $n_{\mathrm{ch}}^{\mathrm{AA}}$ over values for critical density $n_{\mathrm{ch}}^{\mathrm{c,AA}}$ at $\sqrt{s_{NN}} \gtrsim 10$ TeV even with taking into account large statistical uncertainty for $n_{\mathrm{ch}}^{\mathrm{c,AA}}(\sqrt{s_{NN}})$. Thus there is possibility for Bose – Einstein condensation and novel effects, in particular, pion laser in nucleus-nucleus collisions at FCC energy. It seems the theoretical and experimental developments are essential for future progress in this field as well as for more definite conclusions due to improvement of precision for appropriate quantities.

The generalized parametrization for two-particle BEC correlation function is suggested and it takes into account the expansion in closed system of orthogonal polynomials for general case of non-isotropic central-symmetrical Lévy – Feldheim distribution. Possibly, the view of BEC CF can be useful for detailed study of correlation peak shape at FCC.

ACKNOWLEDGMENTS

The author is grateful to Prof. E. K. G. Sarkisyan for fruitful discussions and helpful comments.

CONFLICT OF INTERESTS

The author declares that there is no conflict of interests regarding the publication of this paper.

[1] R. M. Weiner, *Introduction to Bose–Einstein correlations and subatomic interferometry* (John Wiley & Sons Ltd., Chichester and New York, 2000).

[2] R. Hanbury-Brown and R. Q. Twiss, Phil. Mag. **45**, 663 (1954); Nature **177**, 27 (1956); **178**, 1046 (1956).

[3] M. Schaumann, (2015), 1503.09107 [physics.acc-ph].

[4] N. Armesto and et al., Nucl. Phys. A **931**, 1163 (2014); A. Dainese and et al., (2016), 1605.01389 [hep-ph].

[5] N. Armesto and et al., (2016), 1601.02963 [hep-ph].

[6] N. Chang and et al., Sci. China Phys. Mech. Astron. **59**, 621001 (2016).

[7] Z. Fodor and S. D. Katz, J. High Energy Phys. **0302**, 014 (2002).

[8] V. A. Okorokov and E. V. Sandrakova, Univ. J. Phys. App. **1**, 196 (2013).

[9] V. A. Okorokov, (2013), 1312.4269 [nucl-ex].

[10] S. E. Vance, T. Csörgó, and D. Kharzeev, Phys. Rev. Lett. **81**, 2205 (1998).

[11] S. Pratt, Phys. Lett. B **301**, 159 (1993).

[12] S. Pratt, Phys. Rev. C **50**, 469 (1994).

[13] V. A. Okorokov, (2016), 1605.02927 [hep-ph].

[14] Y. Sinyukov, in *Hot hadronic matter: theory and experiment*, NATO ASI Series B, Vol. 346, edited by J. Letessier, H. G. Gutbrod, and J. Rafelski (Plenum Publishing Corp., New York, 1995) p. 309; S. V. Akkelin and Y. M. Sinyukov, Phys. Lett. B **356**, 525 (1995).

[15] S. Pratt, Phys. Rev. D **33**, 1314 (1986); G. F. Bertsch, M. Gong, and M. Tohyama, Phys. Rev. C **37**, 1896 (1988).

[16] U. A. Wiedemann and U. Heinz, Phys. Rep. **319**, 145 (1999).

[17] V. A. Okorokov and E. V. Sandrakova, *Fractals in fundamental physics. Fractal properties of multiparticle production and topology of sample* (MEPhI, Moscow, 2009).

[18] V. A. Okorokov, Adv. High Energy Phys. **2015**, 790646 (2015).

[19] L. Valentin, *Subatomic physics: nuclei and particles. V. I.* (Ermann, Paris, 1982); K. N. Mukhin, *Experimental nuclear physics. V. I.* (Energoatomizdat, Moscow, 1983).

[20] V. A. Okorokov, in *Proc. WPCF 2014*, edited by T. Csörgó, M. Csanád, and T. Novák (Scientific Publishing Services at SLAC) eConf C140825.8 `http://www.slac.stanford.edu/econf/C140825.8/` (2015), 1504.08336 [nucl-ex].

[21] G. Alexander and V. A. Okorokov, J. Phys.: Conf. Ser. **675**, 022001 (2016); (2016), 1610.05298 [hep-ph].

[22] F. Antinori and et al. (WA97), J. Phys. G: Nucl. Part. Phys. **27**, 2325 (2001).

[23] J. Adam and et al. (ALICE), Phys. Rev. C **91**, 034906 (2015).
[24] M. K. Köhler, (2016), 1601.05632 [nucl-ex].
[25] E. V. Shuryak, *The QCD vacuum, hadrons and superdense matter* (World Scientific Publishing Co. Pte. Ltd., Singapore, 2004).
[26] E. K. G. Sarkisyan and A. S. Sakharov, CERN-PH-TH-2004-213 (2004), hep-ph/0410324; AIP Conf. Proc. **828**, 35 (2006); Eur. Phys. C **70**, 533 (2010).
[27] E. K. G. Sarkisyan and et al., Phys. Rev. D **93**, 054046 (2016).
[28] B. I. Abelev and et al. (STAR), Phys. Rev. C **79**, 034909 (2009).
[29] L. J. Gutay and et al., Int. J. Mod. Phys. E **24**, 1550101 (2015).
[30] J. Cleymans and et al., J. Phys. G: Nucl. Part. Phys. **32**, S165 (2006); Phys. Rev. C **73**, 034905 (2006).
[31] W. Li, Mod. Phys. Lett. A **27**, 1230018 (2012); P. Bozek, Phys. Rev. C **85**, 014911 (2012); P. Bozek and W. Broniowski, Phys. Lett. B **718**, 1557 (2013); J. D. Bjorken, S. J. Brodsky, and A. S. Goldhaber, **726**, 344 (2013); K. Dusling and R. Venugopalan, Phys. Rev. D **87**, 051502 (2013); **87**, 054014 (2013); B. Schenke and R. Venugopalan, Phys. Rev. Lett. **113**, 102301 (2014); K. Dusling, W. Li, and B. Schenke, Int. J. Mod. Phys. E **25**, 1630002 (2016).
[32] V. Khachatryan and et al. (CMS), J. High Energy Phys. **0910**, 091 (2010); G. Aad and et al. (ATLAS), Phys. Rev. Lett. **116**, 172301 (2016); V. Khachatryan and et al. (CMS), **116**, 172302 (2016).
[33] I. M. Dremin and J. W. Gary, Phys. Rep. **301**, 349 (2001).
[34] E. Abbas and et al. (ALICE), Phys. Lett. B **726**, 610 (2013).
[35] M. M. Aggarwal and et al. (STAR), Phys. Rev. C **83**, 064905 (2011).
[36] K. Aamodt and et al. (ALICE), Phys. Rev. D **84**, 112004 (2011).
[37] K. Aamodt and et al. (ALICE), Eur. Phys. C **68**, 89 (2010).
[38] J. Adam and et al. (ALICE), (2015), 1509.07541 [nucl-ex].
[39] J. F. Grosse-Oetringhaus and K. Reygers, J. Phys. G: Nucl. Part. Phys. **37**, 083001 (2010).
[40] A. Heister and et al. (ALEPH), Eur. Phys. J. C **35**, 457 (2004).
[41] R. Nouicer and et al. (PHOBOS), J. Phys. G: Nucl. Part. Phys. **30**, S1133 (2004).
[42] G. J. Alner and et al. (UA5), Z. Phys. C **33**, 1 (1986); R. E. Ansorge and et al. (UA5), **43**, 357 (1989).
[43] T. Alexopoulos and et al. (E735), Phys. Rev. D **48**, 1931 (1993); L. Lovás, *The Bose-Einstein correlations in CDFII experiment*, PhD dissertation, Bratislava (2008).
[44] V. Khachatryan and et al. (CMS), Phys. Rev. Lett. **105**, 032001 (2010).
[45] T. Csörgó and J. Zimányi, Phys. Rev. Lett. **80**, 916 (1998); T. Csörgó, Heavy Ion Phys. **9**, 161 (1999); J. Zimányi and T. Csörgó, **9**, 241 (1999).
[46] S. V. Akkelin and Y. M. Sinyukov, Nucl. Phys. A **661**, 613c (1999).
[47] W. Q. Chao, C. S. Gao, and Q. H. Zhang, J. Phys. G: Nucl. Part. Phys. **21**, 847 (1995).
[48] T. Csörgó, S. Hegyi, and W. A. Zajc, Eur. Phys. J. C **36**, 67 (2004).
[49] V. Feller, *An inroduction to probability theory and it's applications* (John Wiley & Sons, New York, 1975); V. M. Zolotarev, *One-dimensional stable distributions* (Nauka, Moscow, 1983).
[50] G. Samorodnitzky and M. S. Taqqu, *Stable non-gaussian random processes* (Chapman & Hall, New York, 1994).
[51] V. V. Uchaikin, Zh. Eksp. Teor. Fiz. **124**, 903 (2003), [JETP **97**, 810 (2003)].
[52] H. B. Stahl and V. Totik, *General orthogonal polynomials* (Cambridge Univ. Press, Cambridge, 1992); A. P. Magnus, (1996), math/9611218; E. Levin and D. S. Lubinsky, *Orthogonal polynomials for exponential weights* (Springer, New York, 2001); T. Kasuda and R. Sakai, J. Approx. **121**, 13 (2003).
[53] A. P. Prudnikov, Y. A. Brichkov, and O. E. Marichev, *Integrals and serieses. Elementary functions* (Nauka, Moscow, 1981).
[54] T. Novák and et al., (2016), 1604.05513 [physics.data-an].
[55] T. Csörgó and S. Hegyi, Phys. Lett. B **489**, 15 (2000).
[56] J. Adams and et al. (STAR), Phys. Rev. C **71**, 044906 (2005); H. C. Eggers, B. Buschbeck, and F. J. October, (2005), hep-ex/0511050; B. Abelev and et al. (ALICE), Phys. Lett. B **739**, 139 (2014); Phys. Rev. C **89**, 024911 (2014).